Electronic Supplementary Material (ESI) for CrystEngComm.
This journal is © The Royal Society of Chemistry 2014

Effect of High Pressure on the Crystal Structure and Properties of (2-fluoro-3-pyridyl)(4-iodophenyl)borinic 8-oxyquinolinate complex

SUPLEMENTARY INFORMATIONS

Grzegorz Wesela-Bauman,[a,b] * Simon Parsons,[c] Janusz Serwatowski,[a] Krzysztof Woźniak[b]

[a] *Physical Chemistry Department, Faculty of Chemistry, Warsaw University of Technology, Noakowskiego 3, 00-664 Warszawa, Poland*
[b] *Laboratory of Crystallochemistry, Department of Chemistry, University of Warsaw, Pasteura 1, 02-093 Warszawa, Poland*
[c] *School of Chemistry and Centre for Science at Extreme Conditions, The University of Edinburgh, King's Buildings, West Mains Road, Edinburgh EH9 3JJ, Scotland.*

*Corresponding authors: grzegorz.wesela@chem.uw.edu.pl

Table of content:

Details on X-ray crystallography

Table S1. Refinement details

Experimental details	**(1) T= 296 K ambient**	**(2) T= 296 K P = 0.17 GPa**	**(3) T= 296 K P = 1.09 GPa**	**(4) T= 296 K P = 2.03 GPa**
Chemical formula	$C_{20}H_{13}BFIN_2O$	$C_{20}H_{13}BFIN_2O$	$C_{20}H_{13}BFIN_2O$	$C_{20}H_{13}BFIN_2O$
M_r	454.03	454.03	454.03	454.03
Crystal system	Monoclinic	Monoclinic	Monoclinic	Monoclinic
space group	$P2_1/n$	$P2_1/n$	$P2_1/n$	$P2_1/n$
Cell settings: a,b,c (Å)	6.8581(2) 14.7849(4) 17.3015(6)	6.8234(4) 14.7074(7) 17.200(2)	6.6545(2) 14.3261(5) 16.7183(14)	6.5502(4) 14.1051(7) 16.497(3)
α,β,γ (°)	90.000 90.966(2) 90.000	90.000 90.814(7) 90.000	90.000 90.460(5) 90.000	90.000 90.396(8) 90.000
V (Å^3)	1754.06(9)	1725.9(2)	1593.75(15)	1524.1(3)
Z	4	4	4	4
d (Mg·m^{-3})	1.719	1.747	1.892	1.979
Radiation type	Mo $K\alpha$	Mo $K\alpha$	Mo $K\alpha$	Mo $K\alpha$
Crystal form,	block , green	block , green	block, green	block, green
Crystal size (mm)	0.20x0.20x0.25	0.20x0.20x0.25	0.20x0.20x0.25	0.20x0.20x0.25
Diffractometer	Bruker APEX II	Bruker APEX II	Bruker APEX II	Bruker APEX II
Data collection	Ω scan	Ω scan	Ω scan	Ω scan
Absorption	Multi-scan	Multi-scan	Multi-scan	Multi-scan
T_{min}, T_{max}	0.62, 0.69	0.60, 0.69	0.59, 0.67	0.57, 0.65
No. of measured, independent and observed [$F^2>2\sigma(F^2)$]	34795 5362 2650	9268 1184 936	8787 1141 887	7648 1067 871
Criterion for observed reflection	I > 2.00σ(I)	I > 2.00σ(I)	I > 2.00σ(I)	I > 2.00σ(I)
Completeness (%)	100	37	39	38
R_{int} (%)	6.5	5.6	4.3	4.0
Θ_{max}	30.53	25.38	25.38	25.38
Range of h,k,l	−9 =< h =< 9 −20 =< k =< 21 −24 =< l =< 24	−7 =< h =< 7 −17 =< k =< 17 −7 =< l =< 7	−8 =< h =< 8 −17 =< k =< 17 −8 =< l =< 8	−7 =< h =< 7 −16 =< k =< 16 −7 =< l =< 7
Refinement on	F	F	F	F
R[$F^2>2\sigma(F^2)$],	0.0510	0.0501	0.0354	0.0326
wR(F^2),	0.0512	0.0396	0.0385	0.0348
GooF	1.000	1.000	1.000	1.000
No. of reflections	2650	936	887	871
No. of parameters	110	110	110	110
$\Delta\rho_{max}$, $\Delta\rho_{min}$	0.70, −0.781	0.40, −0.40	0.58, −0.43	0.37, −0.30
$\Delta / \hat{\sigma}_{max}$	0.0004	0.0002	0.0004	0.0003

Experimental details	**(5) T = 296 K P = 3.02 GPa**	**(6) T= 296 K P =3.96 GPa**	**(7) T= 296 K P = 4.88 GPa**
Chemical formula	$C_{20}H_{13}BFIN_2O$	$C_{20}H_{13}BFIN_2O$	$C_{20}H_{13}BFIN_2O$
M_r	454.03	454.03	454.03
Crystal system space group	Monoclinic $P2_1/n$	Monoclinic $P2_1/n$	Monoclinic $P2_1/n$
Cell settings: a,b,c (Å)	6.4636(2) 13.8775(5) 16.3094(16)	6.4012(4) 13.7152(9) 16.187(3)	6.3469(5) 13.6039(10) 16.105(3)
α,β,γ (°)	90.000 90.317(5) 90.000	90.000 90.438(8) 90.000	90.000 90.549(10) 90.000
V (Å^3)	1462.91(16)	1421.1(3)	1390.5(3)
Z	4	4	4
d (Mg·m^{-3})	2.061	2.122	2.169
Radiation type	Mo $K\alpha$	Mo $K\alpha$	Mo $K\alpha$
Crystal form,	block , green	block , green	block , green
Crystal size (mm)	0.20x0.20x0.25	0.20x0.20x0.25	0.20x0.20x0.25
Diffractometer	Bruker APEX II	Bruker APEX II	Bruker APEX II
Data collection	Ω scan	Ω scan	Ω scan
Absorption	Multi-scan	Multi-scan	Multi-scan
T_{min}, T_{max}	0.56, 0.64	0.56, 0.63	0.57, 0.63
No. of measured, independent and observed [$F^2>2\sigma(F^2)$]	8296 4171 949	6840 1142 916	6772 1187 910
Criterion for observed reflection	I > 2.00σ(I)	I > 2.00σ(I)	I > 2.00σ(I)
Completeness (%)	42	44	46
R_{int} (%)	4.3	4.4	5.7
Θ_{max}	25.33	25.35	25.54
Range of h,k,l	−7 =< h =< 7 −16 =< k =< 16 −8 =< l =< 8	−6 =< h =< 6 −16 =< k =< 16 −9 =< l =< 9	−6 =< h =< 6 −16 =< k =< 16 −10 =< l =< 10
Refinement on	F	F	F
R[$F^2>2\sigma(F^2)$]	0.0339	0.0340	0.0392
wR(F^2)	0.0355	0.0367	0.0417
GooF	1.000	1.000	1.000
No. of reflections	949	916	910
No. of parameters	110	110	110
$\Delta\rho_{max}$, $\Delta\rho_{min}$	0.46, −0.33	0.34, −0.50	0.52, −0.66
Δ/σ_{max}	0.0003	0.0003	0.0002

Data quality for all the pressure steps was sufficient enough to perform anisotropic refinement of the ADPs for all the atoms (not just for the iodine atom). The reason why we present a different model is the low values of reflections to parameters ratios for that sort of refinements.

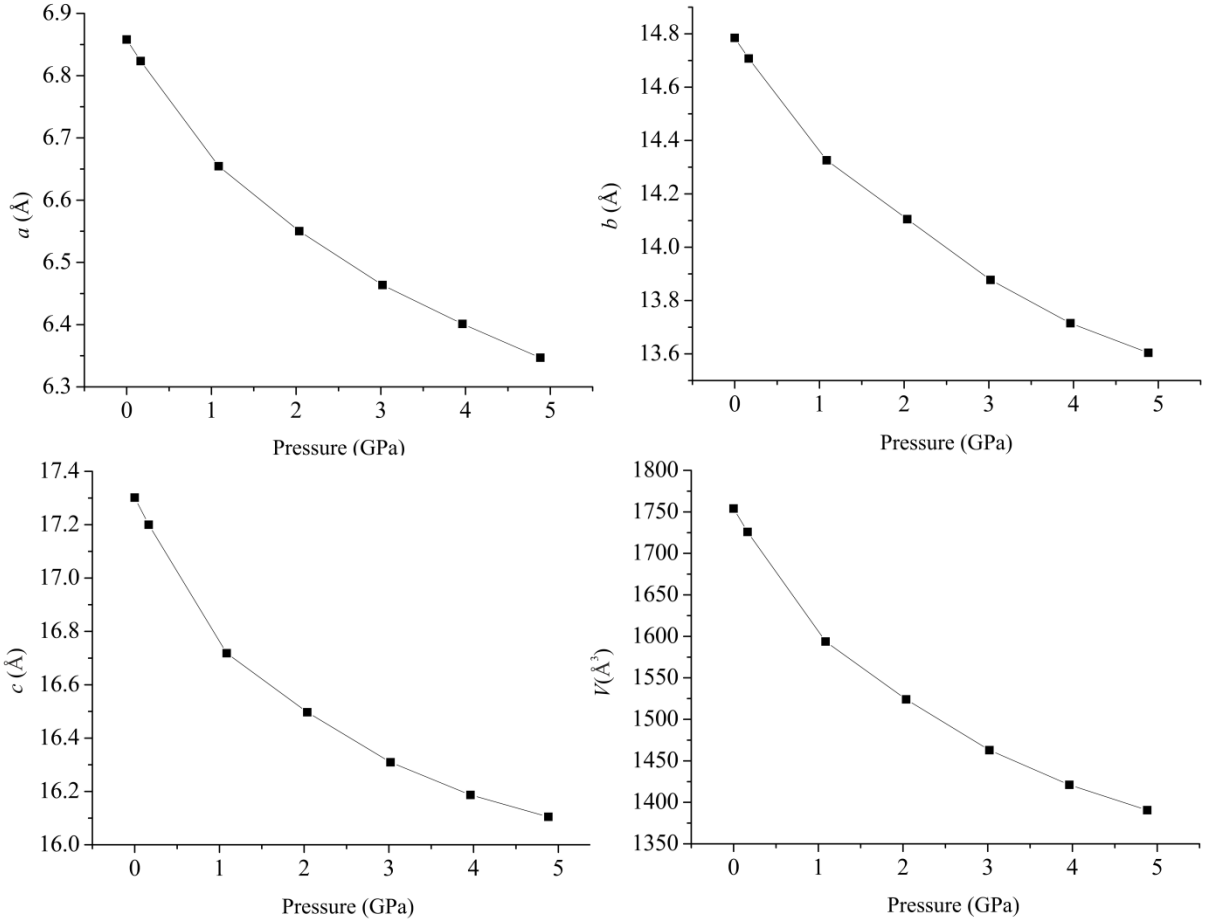

Figure S1. Variation of lattice parameters *a*, *b*, *c* (Å) and volume (Å^3) of **1** as a function of pressure (GPa).

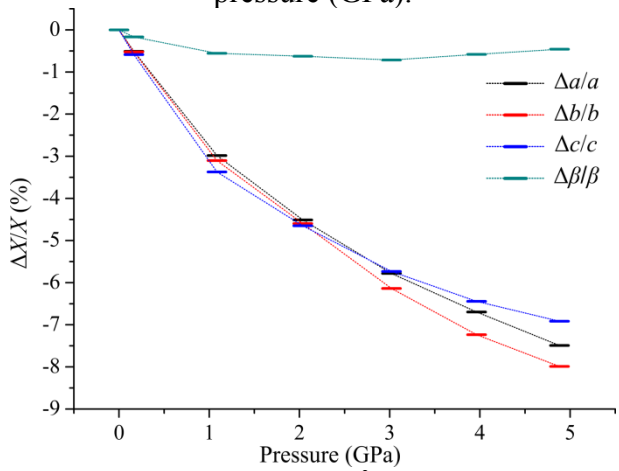

Figure S2. Variation of lattice parameters *a*, *b*, *c* (Å) and *β* (°) of **1** as a function of pressure.

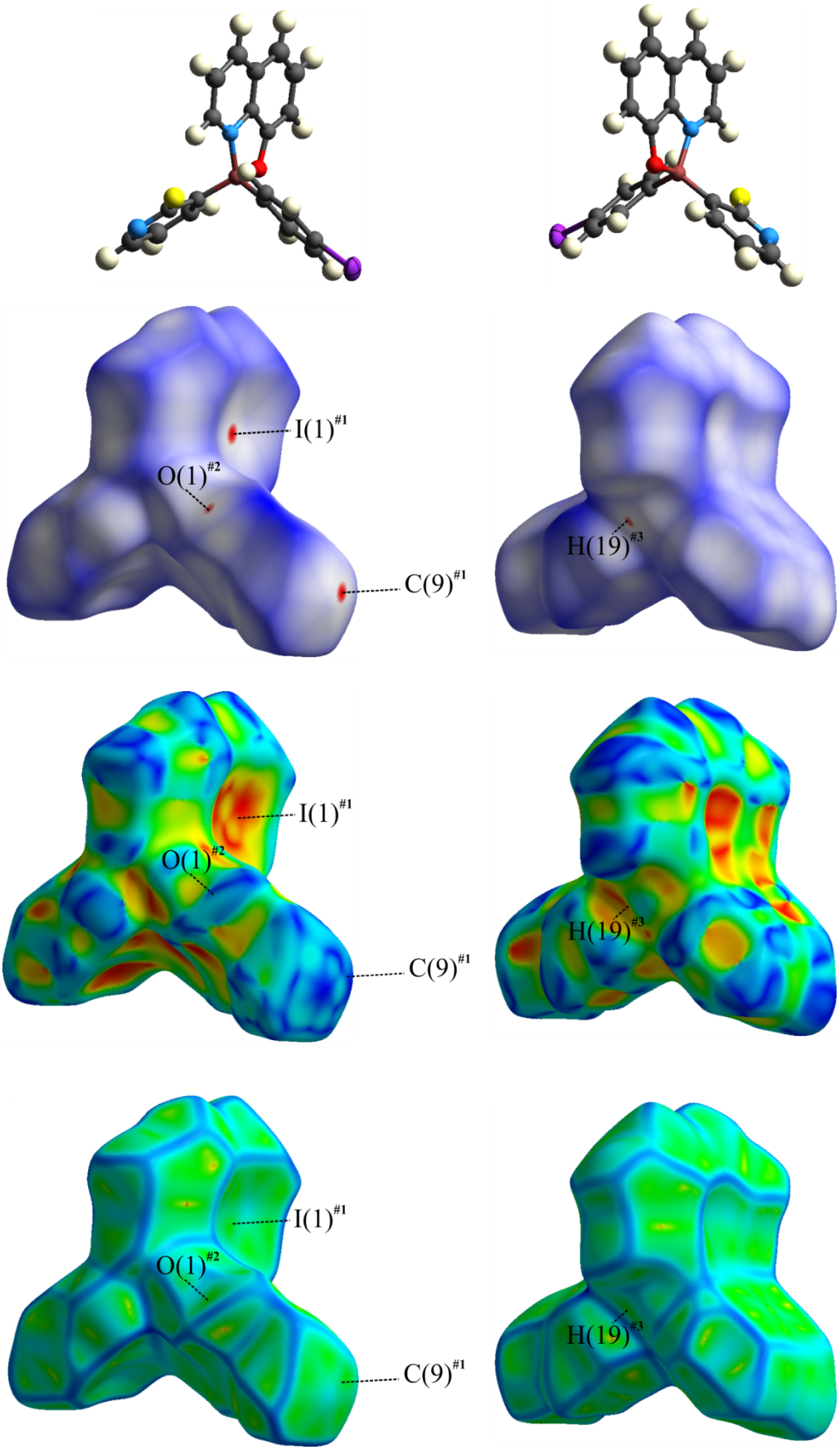

Figure S3. Hirshfeld surface of **1** at ambient pressure (Symmetry operator: #1 1−x,−y,1−z; #2 1+x,y,z; #3 −1+x,y,z).

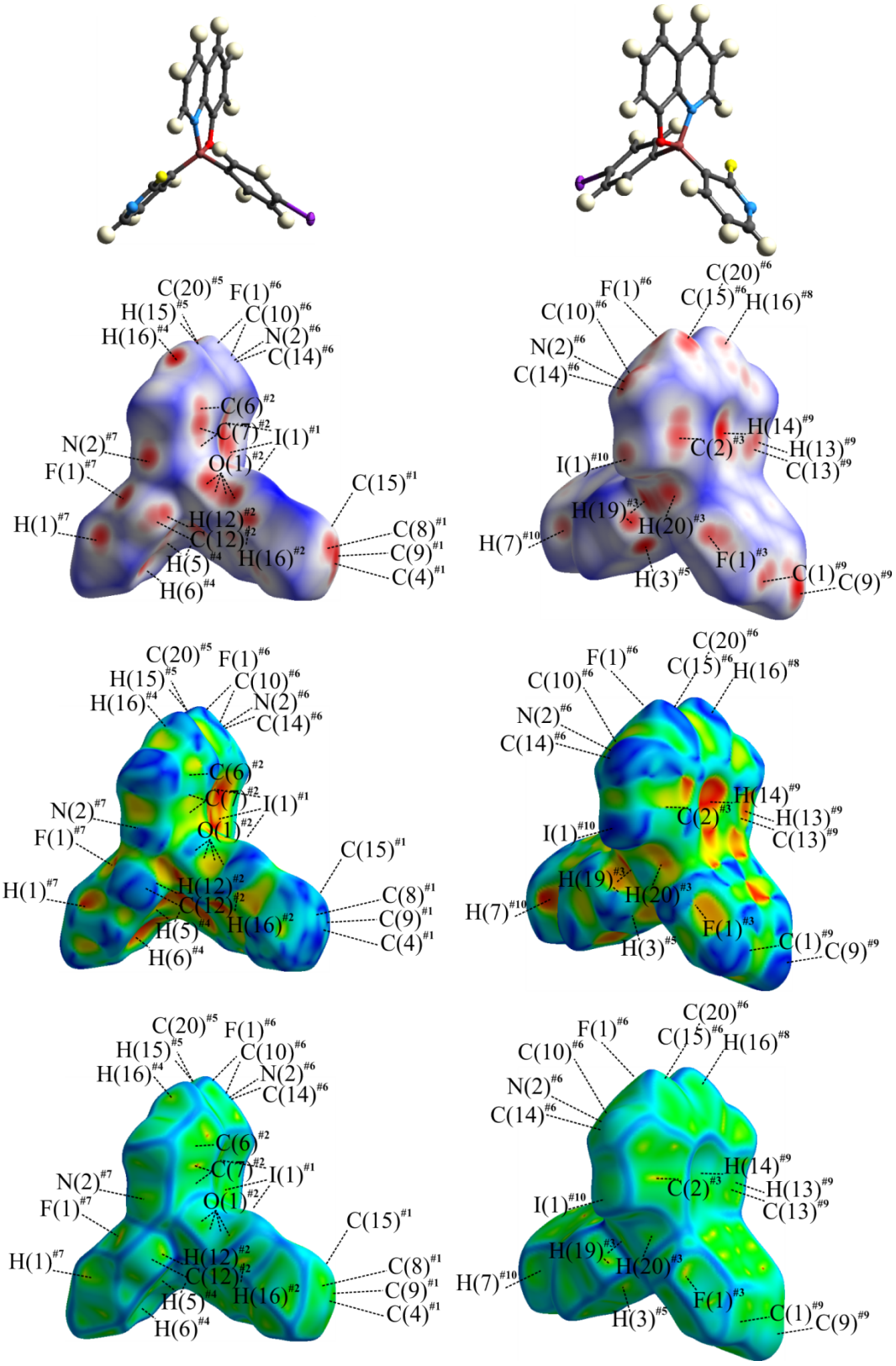

Figure S4. Hirshfeld surface of **1** at 4.9 GPa (Symmetry operators: #1 1−x,−y,1−z; #2 1+x,y,z; #3 −1+x,y,z; #4 0.5+x,1.5−y,0.5+z; #5 −0.5+x,1.5−y,0.5+z; #6 −0.5+x,1.5−y,−0.5+z; #7 −x,2−y,1−z; #8 0.5+x,1.5−y, −0.5+z; #9 −x,2−y,1−z; #10 −x,1−y,1−z).

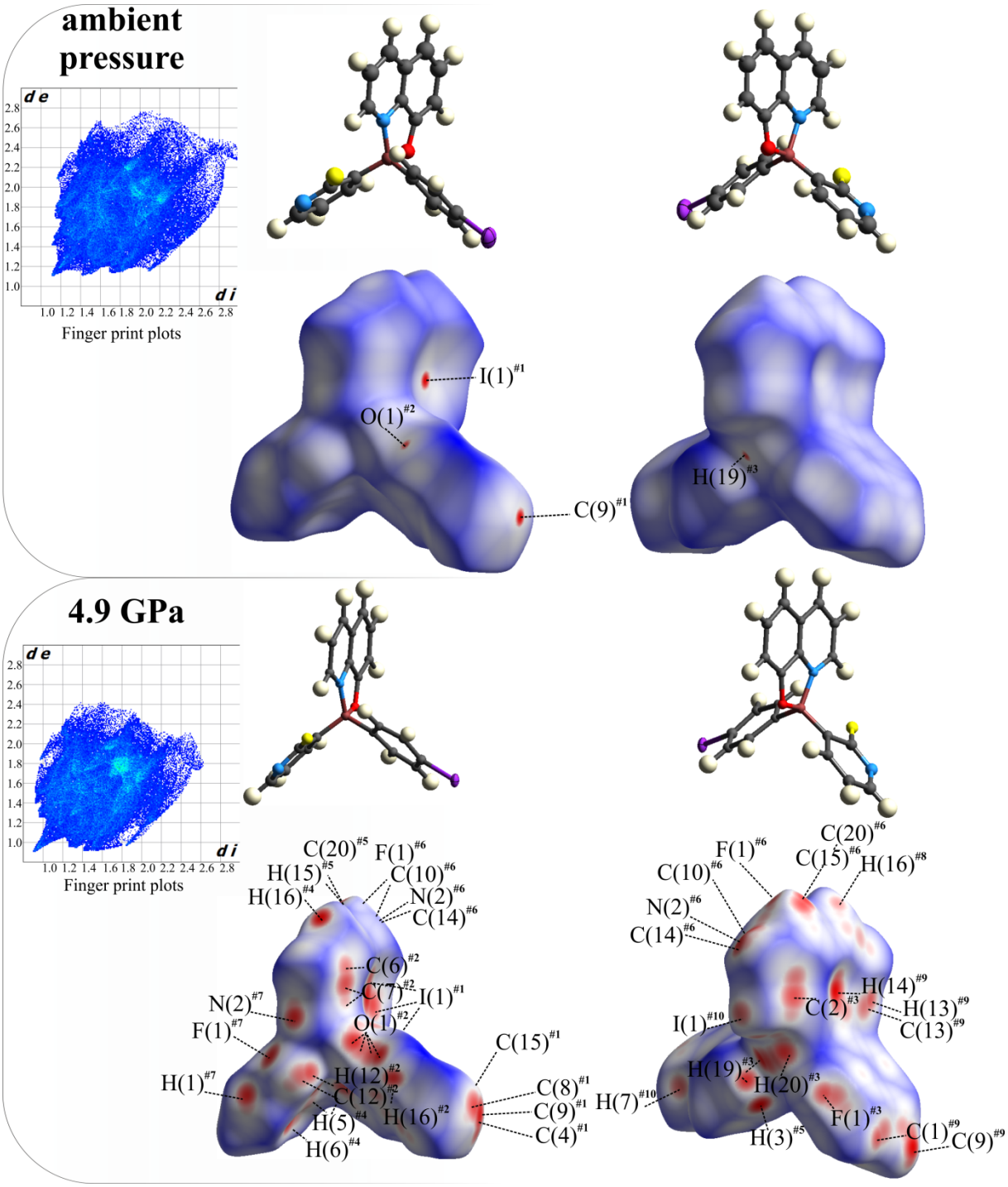

Figure S5. Hirshfeld surface (d_{norm}) of **1** at ambient pressure and at 4.9 GPa (Symmetry operators: #1 1−x,−y,1−z; #2 1+x,y,z; #3 −1+x,y,z; #4 0.5+x,1.5−y,0.5+z; #5 −0.5+x,1.5−y,0.5+z; #6 −0.5+x,1.5−y,−0.5+z; #7 −x,2−y,1−z; #8 0.5+x,1.5−y, −0.5+z; #9 −x,2−y,1−z; #10 −x,1−y,1−z).

Compression of the crystal creates intermolecular contacts involving the 2-fluoro-3-pyridine ring. Fingerprint plots show the distance from the Hirshfeld surface to the nearest nucleus inside of the surface (d_i) and from the Hirshfeld to the nucleus outside of the surface (d_e). Contraction of the crystal contacts is clearly visible by a general shift of the plot to smaller d_e/d_i values. The longer contacts outside the surface (d_e) are decreased between the ambient pressure (*ca* 2.8 Å) and 4.9 GPa (2.4-2.6 Å). A similar compression is observed for the d_i type contacts (from 3.0 Å to 2.6 Å). Short contacts were also affected by high pressure but in a

different manner. This is expressed by round-shape of the high pressure fingerprint. The biggest spike reserved for H...H contacts is more pronounced at 4.9 GPa.

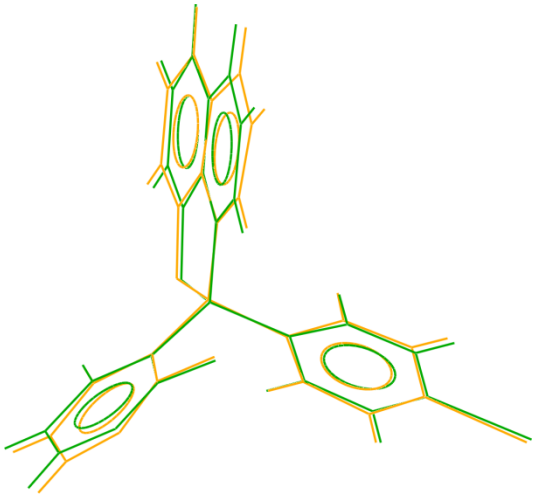

Figure S6. Geometry of **1** at ambient (green) and 4.9 GPa pressure (yellow).

Table S5. Geometry of boron sphere of coordinance (Å and º). Presented atoms were refined anisotropically for better interatomic distances. The results of this particular refinement are not discussed any were else in the manuscript and Supporting Information.

d (A-B) / *P* (GPa)	ambient	0.17	1.09	2.04	3.02	3.96	4.88
B(1)-N(1)	1.634(6)	1.60(3)	1.58(2)	1.60(2)	1.58(2)	1.54(2)	1.59(2)
B(1)-O(1)	1.510(6)	1.51(1)	1.485(9)	1.50(1)	1.503(8)	1.480(9)	1.49(1)
B(1)-C(11)	1.614(7)	1.64(2)	1.62(2)	1.61(1)	1.62(1)	1.62(1)	1.60(1)
B(1)-C(15)	1.609(6)	1.64(2)	1.65(1)	1.61(1)	1.62(1)	1.61(1)	1.60(1)
	ambient	0.17	1.09	2.04	3.02	3.96	4.88
C(11)-B(1)-C(15)	114.7(4)	111(1)	110.9(8)	113.5(8)	111.7(6)	111.7(7)	112.3(8)
C(15)-B(1)-O(1)	109.6(3)	109(1)	108.0(8)	109.5(8)	109.6(6)	109.9(7)	110.0(8)
O(1)-B(1)-N(1)	99.1(3)	101(1)	103.7(8)	100.7(7)	101.0(6)	103.0(7)	100.9(7)
N(1)-B(1)-C(11)	108.9(3)	115(1)	116.6(8)	114.9(8)	116.3(6)	115.6(7)	116.1(8)
C(11)-B(1)-O(1)	114.7(4)	108(1)	107.1(8)	107.7(8)	107.1(6)	107.0(7)	106.8(7)
C(15)-B(1)-N(1)	109.3(3)	112(1)	110.1(8)	109.7(8)	110.4(6)	109.2(7)	110.1(7)

Tensor calculations

Tensor analysis was performed as followed with the *PASCAL*[1] program:

1) Orthonormalization matrixes (M) that transform crystallographic axes (A) to orthogonal axes (E) were calculated for all pressure steps assuming. Assuming **E** = **MA** the general formula for such transformation is:

$$M = \begin{vmatrix} 0.9049 & 0.0000 & -0.4256 \\ 0.0000 & -1.0000 & 0.0000 \\ -0.9479 & 0.0000 & -0.3185 \end{vmatrix}$$

which indicates that $X_1 \sim a$, $X_2 = -b$

2) The strain tensors (e) were evaluated according to:

$$\mathbf{e_i = (M_i^T)^{-1}M_0^T - I}$$

,where I is the unit matrix, M_0 is the transformation for the ambient pressure unit cell, and M_i is the transformation for subsequent pressure steps). The Lagrangian infinitesimal strain tensors (ε_i) were calculated with:

$$\boldsymbol{\varepsilon_i = 0.5[(M_i^T)^{-1}M_0^T + M_0(M^T)^{-1}] - I}$$

,and Lagrangian finite strain tensors (η_i) were calculated with:

$$\boldsymbol{\eta_i = 0.5(e_i + e_i^T + e_i e_i^T)}$$

3) K_{1i}, K_{2i} and K_{3i} were calculated using empirical fitting of the formula:

$$\mathbf{x(p) = x_0 + k|p - p_c|^A}$$

Compressibility (TPa^{-1})

P **(GPa)**	K_1	K_2	K_3	$\sigma(K_1)$	$\sigma(K_2)$	$\sigma(K_3)$
0.00	58.72	41.90	35.15	13.32	10.45	4.78
0.16	45.09	36.02	30.63	4.32	5.07	2.43
1.09	20.27	20.22	17.84	1.11	1.36	0.65
2.04	13.19	13.94	12.48	0.47	0.76	0.39
3.02	9.79	10.57	9.53	0.44	0.52	0.25
3.96	7.88	8.58	7.77	0.61	0.85	0.42
4.88	6.65	7.26	6.59	0.74	1.14	0.58

Birch-Murnaghan Coefficients

	B_0 **(GPa)**	$\sigma(B_0$ **(GPa))**	V_0 **(Å^3)**	$\sigma(V_0$ **(Å^3))**	**B'**	**σ(B')**
2nd	13.6023	1.0776	1729.8946	16.8856	4	n/a
3rd	6.7036	0.9697	1759.4086	10.0658	11.1893	1.6202

P **(GPa)**	P_{lin}	$P_{calc,2nd}$	P_{3rd}	***V*** **(Å^3)**
0.00	−0.3751	−0.1835	0.0208	1754.0591
0.16	−0.0193	0.0314	0.1432	1725.9227
1.09	1.6518	1.3137	1.1049	1593.7549
2.04	2.5321	2.2195	1.9774	1524.1417
3.02	3.3063	3.1901	3.0547	1462.9081
3.96	3.8352	3.9666	4.0084	1421.0757
4.88	4.2221	4.6023	4.8439	1390.4836

	% change in length		
P **(GPa)**	X_1	X_2	X_3
0.00	0.0000	0.0000	0.0000
0.16	−0.6798	−0.5228	−0.4054
1.09	−3.5699	−3.0550	−2.6548
2.04	−4.9172	−4.4922	−3.9981
3.02	−6.0732	−5.9490	−5.0665
3.96	−6.9734	−6.7459	−5.9150
4.88	−7.6688	−7.3220	−6.5201

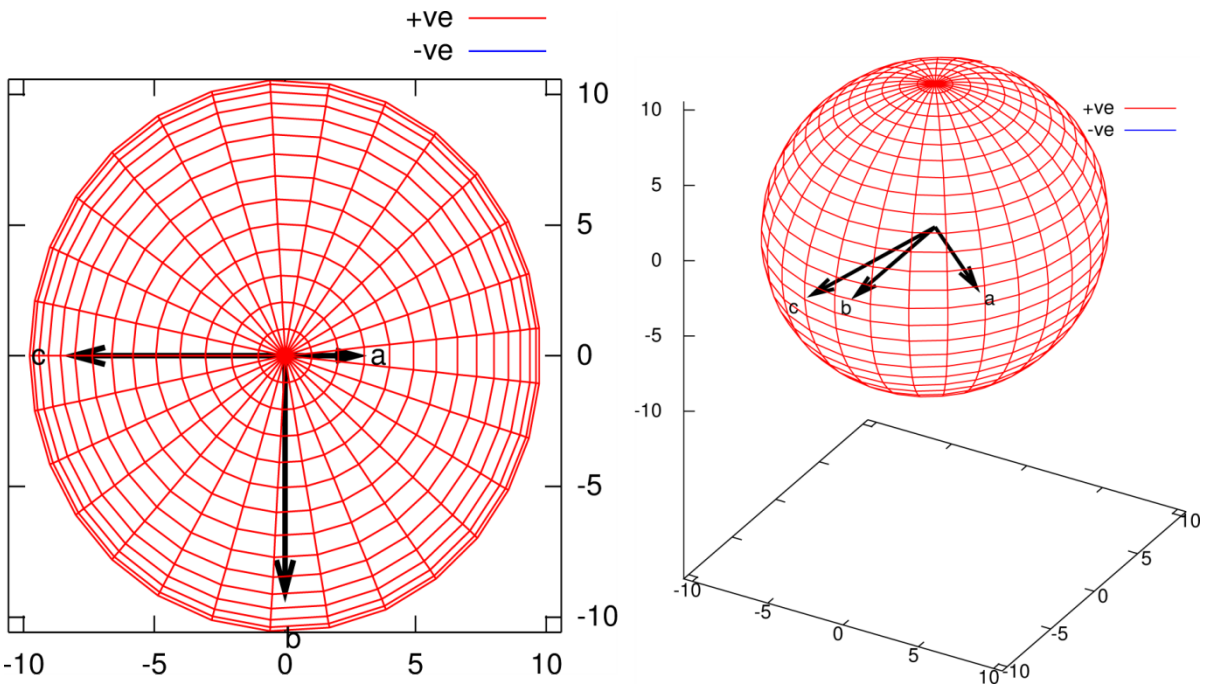

Figure S7. Tensor of compressibility calculated for orthogonal axes.

As a comparisment the data gather for $Ru_3(CO)_{12}$ and L-alanine (up to *ca* 5 GPa)[2,3] analysis done in *PASCAL* proved that those materials are not undergoing rapid stiffening with increasing pressure as much as compound **1** and, what is more, their compression is anisotropic.

Strain calculations

Strain analysis was performed with the *STRAIN*[4–6] program. Output of the program is listed below:

Strain tensor calculation

Lattice parameters of cell number 1 (undeformed):

6.8581 14.7849 17.3015 90.000 90.966 90.000

Lattice parameters of cell number 2 (deformed):

6.3469 13.6039 16.1050 90.000 90.549 90.000

Metric tensor M_1:
[47.033536 0.000000 −2.000421]
[0.000000 218.593268 0.000000]
[−2.000421 0.000000 299.341902]
Metric tensor M_2:
[40.283140 0.000000 −0.979412]
[0.000000 185.066095 0.000000]
[−0.979412 0.000000 259.371025]
Standard root tensor R_1:
[6.857125 0.000000 0.000000]
[0.000000 14.784900 0.000000]
[−0.115621 0.000000 17.301500]
Standard root tensor R_2:
[6.346609 0.000000 0.000000]
[0.000000 13.603900 0.000000]
[−0.060814 0.000000 16.105000]

Note: The standard root tensor R of metric tensor $M=R^TR$ transforms fractional direct space coordinates X, into cartesian coordinates X_c such: $X_c = R\ X$

Linear Lagrangian Strain Tensor (small deformation)
[−0.074451 0.000000 0.003413]
[0.000000 −0.079879 −0.000000]
[0.003413 −0.000000 −0.069156]

Eigenvalues
−0.07988 −0.07612 −0.06748

Note: The linear Lagrangian strain tensor can be calculated according to the formula: $S = 0.5 (e + e^T)$, where, $e = R_2R_1^{-1} − I$ and, R_1 and R_2 are the standard root tensors of cell 1 and 2, and I is a 3x3 identity matrix

Finite Lagrangian Strain Tensor (finite deformation)
[−0.071656 0.000000 0.003177]
[0.000000 −0.076688 −0.000000]
[0.003177 −0.000000 −0.066765]

Eigenvalues
−0.07669; −0.07322; −0.06520

Degree of lattice distortion
0.04149

Note: The finite Lagrangian strain tensor can be calculated according to the formula: $S = 0.5 (e + e^T + e^T e)$, where, $e = R_2R_1^{-1} − I$ and, R_1 and R_2 are the standard root tensors of cell 1 and 2, and I is a 3x3 identity matrix

Note: The degree of lattice distortion is described here as the spontaneous strain (square root of the sum of squared eigenvalues of strain tensor) divided by 3

Details on theoretical calculations

***PIXEL*[7–9] calculations**

Table S2. Evaluation of Lattice Energies (E_L) their contributions from Electrostatic (E_{elstat}), Polarization (E_{pol}), Dispersion (E_{disp}), and Repulsion (E_{rep}) terms. Calculated using *PIXEL*.

	Energy (kJ mol^{-1})				
	E_{elstat}	E_{pol}	E_{disp}	E_{rep}	E_L
0	−129.3	−48.4	−199.2	202.4	−174.4
0.16	−144.4	−54.7	−210.5	226.8	−182.8
1.09	−221.6	−87.7	−266.3	387.6	−187.9
2.04	−281.3	−114.2	−308.3	507.5	−196.3
3.02	−354.1	−147.1	−348.7	652.6	−197.2
3.96	−422.1	−177.6	−380.5	794.9	−185.2
4.88	−466.2	−198.9	−405.0	889.0	−180.3

Table S3. Changes of Lattice Energies (E_L) their contributions from Electrostatic (E_{elstat}), Polarization (E_{pol}), Dispersion (E_{disp}), and Repulsion (E_{rep}) terms. Calculated using *PIXEL*.

	Δ*E*/*E* (%)				
	E_{elstat}	E_{pol}	E_{disp}	E_{rep}	E_L
0	0	0	0	0	0
0.16	12%	13%	6%	12%	5%
1.09	71%	81%	34%	92%	8%
2.04	118%	136%	55%	151%	13%
3.02	174%	204%	75%	222%	13%
3.96	226%	267%	91%	293%	6%
4.88	261%	311%	103%	339%	3%

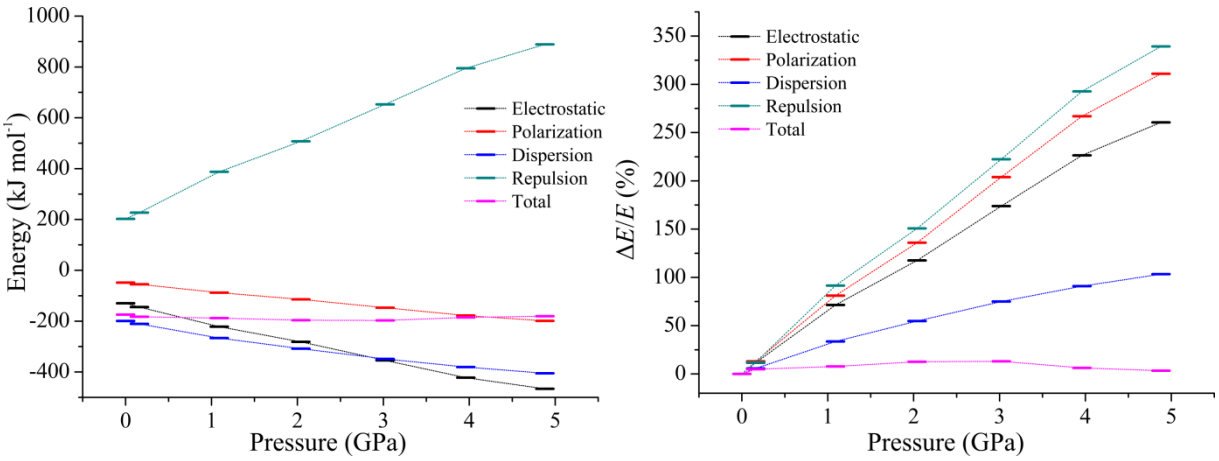

Figure S8. Impact of pressure on lattice energies and contributions from Electrostatic, Polarization, Dispersion, and Repulsion terms. Calculated using *PIXEL*.

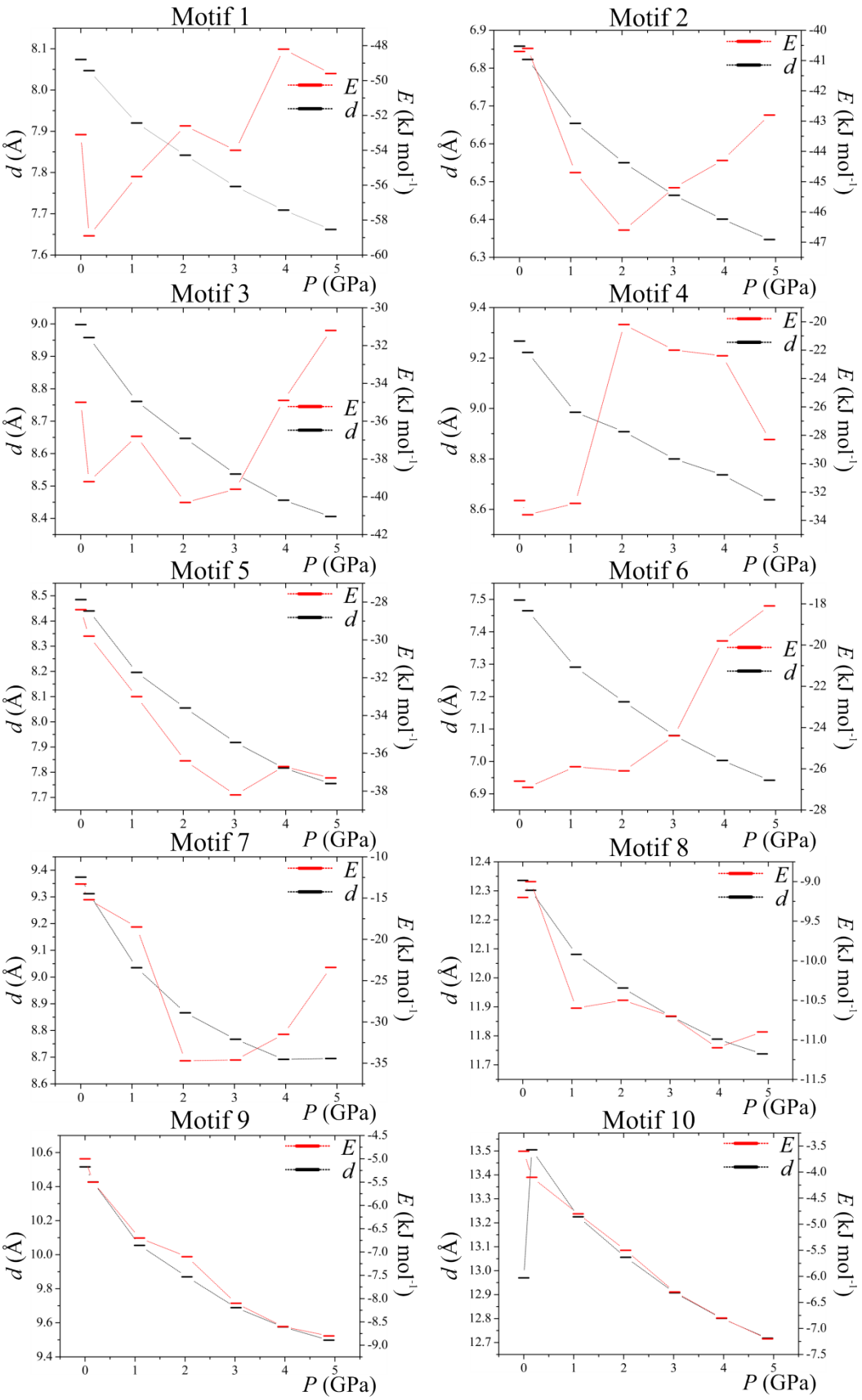

Figure S9. The distances (*d*) between the centre of masses of two interacting molecules and their corresponding energies (*E*) for crystal motifs present in **1** as a function of pressure. Calculated using *PIXEL*.

Table S4. *PIXEL* calculations for ambient conditions

Crystal lattice interactions

Pathways	E / kJ mol^{-1}	symmetry operator	d / Å
1	−53.1	1−x, 1−y, 1−z	8.074
2	−40.7	x±1, y, z	6.858
3	−35.0	1−x, −y, 1−z	8.998
4	−32.6	x±0.5, 0.5−y, z±0.5	9.267
5	−28.4	−x, −y, 1−z	8.485
6	−26.6	−x, 1−y, 1−z	7.498
7	−13.3	x±0.5, 0.5−y, z±0.5	9.374
8	−9.2	0.5−x, y±0.5, 1.5−z	12.336
9	−5.0	0.5−x, y±0.5, 0.5−z	10.516
10	−3.6	2−x, 1−y, 1−z	12.970

Table S5. *PIXEL* calculations for 0.16 GPa.

Crystal lattice interactions

Pathways	E / kJ mol^{-1}	symmetry operator	d / Å
1	−58.9	1−x, 2−y, 1−z	8.047
2	−40.6	x±1, y, z	6.823
3	−39.2	1−x, 1−y, 1−z	8.958
4	−33.6	x±0.5, 1.5−y, z±0.5	9.222
5	−29.8	−x, 1−y, 1−z	8.440
6	−26.9	−x, 2−y, 1−z	7.465
7	−15.2	x±0.5, 1.5−y, z±0.5	9.312
8	−9.0	0.5−x, y±0.5, 1.5−z	12.302
9	−5.5	0.5−x, y±0.5, 0.5−z	10.427
10	−4.1	2−x, 1−y, 1−z	13.505

Table S6. *PIXEL* calculations for 1.09 GPa.

Crystal lattice interactions

Pathways	E / kJ mol^{-1}	symmetry operator	d / Å
1	−55.5	1−x, 2−y, 1−z	7.920
2	−44.7	x±1, y, z	6.654
3	−36.8	1−x, 1−y, 1−z	8.761
4	−32.8	x±0.5, 1.5−y, z±0.5	8.985
5	−33.0	−x, 1−y, 1−z	8.196
6	−25.9	−x, 2−y, 1−z	7.291
7	−18.5	x±0.5, 1.5−y, z±0.5	9.035
8	−10.6	0.5−x, y±0.5, 1.5−z	12.081
9	−6.7	0.5−x, y±0.5, 0.5−z	10.055
10	−4.8	2−x, 1−y, 1−z	13.225

Table S7. *PIXEL* calculations for 2.04 GPa.

Crystal lattice interactions

Pathways	E / kJ mol^{-1}	symmetry operator	d / Å
1	−52.6	1−x, 2−y, 1−z	7.842
2	−46.6	x±1, y, z	6.550
3	−40.3	1−x, 1−y, 1−z	8.647
4	−20.2	x±0.5, 1.5−y, z±0.5	8.908
5	−36.4	−x, 1−y, 1−z	8.055
6	−26.1	−x, 2−y, 1−z	7.184
7	−34.7	x±0.5, 1.5−y, z±0.5	8.866
8	−10.5	0.5−x, y±0.5, 1.5−z	11.965
9	−7.1	0.5−x, y±0.5, 0.5−z	9.870
10	−5.5	2−x, 1−y, 1−z	13.056

Table S8. *PIXEL* calculations for 3.02 GPa.

Crystal lattice interactions

Pathways	E / kJ mol^{-1}	symmetry operator	d / Å
1	−54.0	1−x, 2−y, 1−z	7.766
2	−45.2	x±1, y, z	6.464
3	−39.6	1−x, 1−y, 1−z	8.537
4	−22.0	x±0.5, 1.5−y, z±0.5	8.800
5	−38.2	−x, 1−y, 1−z	7.918
6	−24.4	−x, 2−y, 1−z	7.080
7	−34.6	x±0.5, 1.5−y, z±0.5	8.767
8	−10.7	0.5−x, y±0.5, 1.5−z	11.867
9	−8.1	0.5−x, y±0.5, 0.5−z	9.689
10	−6.3	2−x, 1−y, 1−z	12.908

Table S9. *PIXEL* calculations for 3.96 GPa.

Crystal lattice interactions

Pathways	E / kJ mol^{-1}	symmetry operator	d / Å
1	−48.2	1−x, 2−y, 1−z	7.709
2	−44.3	x±1, y, z	6.401
3	−34.9	1−x, 1−y, 1−z	8.456
4	−22.4	x±0.5, 1.5−y, z±0.5	8.737
5	−36.7	−x, 1−y, 1−z	7.817
6	−19.8	−x, 2−y, 1−z	7.003
7	−31.5	x±0.5, 1.5−y, z±0.5	8.692
8	−11.1	0.5−x, y±0.5, 1.5−z	11.789
9	−8.6	0.5−x, y±0.5, 0.5−z	9.576
10	−6.8	2−x, 1−y, 1−z	12.801

Table S10. *PIXEL* calculations for 4.88 GPa.

Crystal lattice interactions			
Pathways	E / kJ mol^{-1}	symmetry operator	d / Å
1	−49.6	1−x, 2−y, 1−z	7.662
2	−42.8	x±1, y, z	6.347
3	−31.2	1−x, 1−y, 1−z	8.406
4	−28.3	x±0.5, 1.5−y, z±0.5	8.638
5	−37.3	−x, 1−y, 1−z	7.755
6	−18.1	−x, 2−y, 1−z	6.942
7	−23.4	x±0.5, 1.5−y, z±0.5	8.695
8	−10.9	0.5−x, y±0.5, 1.5−z	11.738
9	−8.8	0.5−x, y±0.5, 0.5−z	9.498
10	−7.2	2−x, 1−y, 1−z	12.718
11	−5.0	2−x, 2−y, 1−z	12.238

Charge transfer analysis of 1.

Table S11. Charge transfer analysis for ambient conditions (level of theory B3LYP/6-31+g(d,p))

	Energy (a.u.)			
Pathways	HOMO−1	HOMO	LUMO	LUMO+1
1	−0.225349	−0.225346	−0.090718	−0.090651
2	−0.227691	−0.224004	−0.105123	−0.103535
3	−0.227080	−0.213316	−0.095549	−0.095497
4	−0.220756	−0.216595	−0.109925	−0.085138
5	−0.229523	−0.228487	−0.098070	−0.097671
6	−0.227394	−0.227351	−0.101291	−0.100810
7	−0.230898	−0.222791	−0.108512	−0.095661
8	−0.224800	−0.223128	−0.098686	−0.097073
9	−0.232801	−0.228758	−0.105500	−0.102397

Pathways	H_{AB} (10^{-4} a.u.)		charge transport
	hole	electron	
1	0.015	0.335	electron
2	18.435	7.940	hole
3	68.820	0.260	hole
4	20.805	123.935	electron
5	5.180	1.995	hole
6	0.215	2.405	electron
7	40.535	64.255	electron
8	8.360	8.065	hole
9	20.215	15.515	hole
sum	182.580	224.705	**electron**

Table S12. Charge transfer analysis for ambient conditions (level of theory B97D/6-31+g(d,p))

	Energy (a.u.)			
Pathways	HOMO−1	HOMO	LUMO	LUMO+1
1	−0,195884	−0,195851	−0,109389	−0,109233
2	−0.199150	−0.195226	−0.122706	−0.121345
3	−0.196348	−0.185505	−0.113557	−0.113550
4	−0.191337	−0.186886	−0.127658	−0.103759
5	−0.199117	−0.198380	−0.116237	−0.115865
6	−0.198423	−0.198379	−0.119205	−0.118779
7	−0.199724	−0.194152	−0.126185	−0.114084
8	−0.196077	−0.194422	−0.116784	−0.115150
9	−0.203612	−0.199747	−0.123278	−0.120317

Pathways	$H_{ab.}$ (10^{-4} a.u.)		charge transport
	hole	electron	
1	0.165	0.780	electron
2	19.620	6.805	hole
3	54.215	0.035	hole
4	22.255	119.495	electron
5	3.685	1.860	hole
6	0.220	2.130	electron
7	27.860	60.505	electron
8	8.275	8.170	hole
9	19.325	14.805	hole
sum	155.455	213.805	**electron**

Table S13. Charge transfer analysis for 0.16 GPa (level of theory B3LYP/6-31+g(d,p))

	Energy (a.u.)			
Pathways	HOMO−1	HOMO	LUMO	LUMO+1
1	−0.222949	−0.222922	−0.103211	−0.103070
2	−0.227733	−0.224121	−0.117875	−0.116637
3	−0.222745	−0.212729	−0.108464	−0.108455
4	−0.219059	−0.212112	−0.123380	−0.097403
5	−0.225634	−0.225060	−0.111062	−0.110642
6	−0.226955	−0.226897	−0.113871	−0.113435
7	−0.225441	−0.222474	−0.122132	−0.107887
8	−0.224441	−0.223018	−0.111471	−0.109954
9	−0.231271	−0.228865	−0.118652	−0.115420

	H_{AB} (10^{-4} a.u.)		charge transport
Pathways	hole	electron	
1	0.135	0.705	electron
2	18.060	6.190	hole
3	50.080	0.045	hole
4	34.735	129.885	electron
5	2.870	2.100	hole
6	0.290	2.180	electron
7	14.835	71.225	electron
8	7.115	7.585	electron
9	12.030	16.160	electron
sum	140.150	236.075	**electron**

Table S14. Charge transfer analysis for 0.16 GPa (level of theory B97D/6-31+g(d,p))

	Energy (a.u.)			
Pathways	HOMO−1	HOMO	LUMO	LUMO+1
1	−0.193170	−0.193101	−0.120861	−0.120631
2	−0.199420	−0.195524	−0.134192	−0.133172
3	−0.192692	−0.185231	−0.125374	−0.125322
4	−0.190443	−0.182851	−0.139856	−0.115036
5	−0.195549	−0.195130	−0.128095	−0.127703
6	−0.226955	−0.226897	−0.113871	−0.113435
7	−0.195205	−0.194131	−0.138538	−0.125269
8	−0.194973	−0.194586	−0.128395	−0.126854
9	−0.200794	−0.19990	−0.135188	−0.132124

Pathways	H_{AB} (10^{-4} a.u.)		charge transport
	hole	electron	
1	0.345	1.150	electron
2	19.480	5.100	hole
3	37.305	0.260	hole
4	37.960	124.100	electron
5	2.095	1.960	hole
6	0.290	2.180	electron
7	5.370	66.345	electron
8	1.935	7.705	electron
9	4.470	15.320	electron
sum	108.960	221.940	**electron**

Table S15. Charge transfer analysis for 1.09 GPa (level of theory B3LYP/6-31+g(d,p))

Pathways	Energy (a.u.)			
	HOMO−1	HOMO	LUMO	LUMO+1
1	−0.218936	−0.218920	−0.101530	−0.101356
2	−0.223574	−0.219189	−0.116240	−0.114376
3	−0.218076	−0.204342	−0.106713	−0.106558
4	−0.214027	−0.207012	−0.121673	−0.094983
5	−0.221630	−0.220740	−0.109234	−0.108657
6	−0.222798	−0.222786	−0.112689	−0.112142
7	−0.221706	−0.218083	−0.120516	−0.105981
8	−0.220390	−0.218284	−0.109914	−0.108126
9	−0.226656	−0.224212	−0.116707	−0.112934

Table S16. Charge transfer analysis for 1.09 GPa (level of theory B97D/6-31+g(d,p))

Pathways	Energy (a.u.)			
	HOMO−1	HOMO	LUMO	LUMO+1
1	−0.190197	−0.190156	−0.119115	−0.118855
2	−0.195881	−0.191291	−0.132562	−0.130903
3	−0.189188	−0.177813	−0.123581	−0.123499
4	−0.186130	−0.178861	−0.138190	−0.112615
5	−0.192700	−0.192020	−0.126307	−0.125763
6	−0.194720	−0.194618	−0.129444	−0.128971
7	−0.192656	−0.190372	−0.136938	−0.123375
8	−0.192169	−0.190453	−0.126865	−0.125068
9	−0.197222	−0.196070	−0.133296	−0.129706

Table S17. Charge transfer analysis for 2.04 GPa (level of theory B3LYP/6-31+g(d,p))

	Energy (a.u.)			
Pathways	HOMO−1	HOMO	LUMO	LUMO+1
1	−0.223112	−0.223041	−0.096550	−0.096415
2	−0.228960	−0.224832	−0.111815	−0.110200
3	−0.222269	−0.207483	−0.101676	−0.101639
4	−0.226761	−0.223444	−0.115804	−0.101396
5	−0.226296	−0.225353	−0.104534	−0.103958
6	−0.227597	−0.227593	−0.107960	−0.107340
7	−0.220136	−0.211169	−0.117186	−0.090405
8	−0.225268	−0.223582	−0.105136	−0.103386
9	−0.232205	−0.229421	−0.111905	−0.108442
10	−0.226595	−0.226497	−0.104947	−0.104947

Table S18. Charge transfer analysis for 2.04 GPa (level of theory B97D/6-31+g(d,p))

	Energy (a.u.)			
Pathways	HOMO−1	HOMO	LUMO	LUMO+1
1	−0.223112	−0.223041	−0.096550	−0.096415
2	−0.228960	−0.224832	−0.111815	−0.110200
3	−0.192818	−0.180360	−0.118900	−0.118789
4	−0.226761	−0.223444	−0.115804	−0.101396
5	−0.226296	−0.225353	−0.104534	−0.103958
6	−0.198511	−0.198487	−0.125047	−0.124498
7	−0.220136	−0.211169	−0.117186	−0.090405
8	−0.225268	−0.223582	−0.105136	−0.103386
9	−0.232205	−0.229421	−0.111905	−0.108442
10	−0.226595	−0.226497	−0.104947	−0.104947

Table S19. Charge transfer analysis for 3.02 GPa (level of theory B3LYP/6-31+g(d,p))

	Energy (a.u.)			
Pathways	HOMO−1	HOMO	LUMO	LUMO+1
1	−0.224083	−0.224076	−0.096931	−0.096759
2	−0.225907	−0.222360	−0.113220	−0.111587
3	−0.223811	−0.204402	−0.102740	−0.102721
4	−0.227311	−0.220597	−0.117669	−0.101419
5	−0.228137	−0.226601	−0.105589	−0.104965
6	−0.225999	−0.225658	−0.108441	−0.107747
7	−0.216807	−0.212274	−0.119055	−0.090568
8	−0.222900	−0.220718	−0.105922	−0.104381
9	−0.232496	−0.227756	−0.113349	−0.109702
10	−0.224819	−0.224784	−0.106090	−0.106083

Table S20. Charge transfer analysis for 3.02 GPa (level of theory B97D/6-31+g(d,p))

	Energy (a.u.)			
Pathways	HOMO−1	HOMO	LUMO	LUMO+1
1	−0.194800	−0.194681	−0.114936	−0.114657
2	−0.197748	−0.193883	−0.129810	−0.128269
3	−0.193598	−0.177576	−0.119894	−0.119799
4	−0.196772	−0.192319	−0.134369	−0.119161
5	−0.197669	−0.196714	−0.122946	−0.122350
6	−0.197381	−0.197089	−0.125480	−0.124866
7	−0.188244	−0.182833	−0.135872	−0.108438
8	−0.194496	−0.192373	−0.123165	−0.121597
9	−0.202545	−0.199027	−0.130234	−0.126755
10	−0.196262	−0.196241	−0.123278	−0.123274

Table S21. Charge transfer analysis for 3.96 GPa (level of theory B3LYP/6-31+g(d,p))

	Energy (a.u.)			
Pathways	HOMO−1	HOMO	LUMO	LUMO+1
1	−0.223150	−0.223102	−0.097666	−0.097445
2	−0.227460	−0.223059	−0.114127	−0.111870
3	−0.222296	−0.202120	−0.103437	−0.103395
4	−0.226569	−0.221599	−0.118511	−0.102537
5	−0.226696	−0.225414	−0.106553	−0.105817
6	−0.226516	−0.226221	−0.109699	−0.108902
7	−0.217525	−0.209837	−0.119929	−0.091049
8	−0.223761	−0.221757	−0.106800	−0.105219
9	−0.231983	−0.228285	−0.114065	−0.110139
10	−0.225422	−0.225293	−0.106758	−0.106745

Table S22. Charge transfer analysis for 3.96 GPa (level of theory B97D/6-31+g(d,p))

	Energy (a.u.)			
Pathways	HOMO−1	HOMO	LUMO	LUMO+1
1	−0.193476	−0.193372	−0.115609	−0.115293
2	−0.199307	−0.194649	−0.130594	−0.128497
3	−0.192416	−0.175502	−0.120512	−0.120388
4	−0.196390	−0.193364	−0.135126	−0.120252
5	−0.196663	−0.195659	−0.123876	−0.123173
6	−0.197514	−0.197461	−0.126704	−0.125990
7	−0.189060	−0.180736	−0.136673	−0.108884
8	−0.195206	−0.193454	−0.124002	−0.122389
9	−0.201476	−0.199466	−0.130879	−0.127152
10	−0.196812	−0.196672	−0.123898	−0.123886

Table S23. Charge transfer analysis for 4.88 GPa (level of theory B3LYP/6-31+g(d,p))

	Energy (a.u.)			
Pathways	HOMO−1	HOMO	LUMO	LUMO+1
1	−0.221560	−0.221540	−0.097241	−0.097100
2	−0.224448	−0.221443	−0.114270	−0.111854
3	−0.222125	−0.199448	−0.103847	−0.103787
4	−0.215738	−0.208261	−0.119956	−0.090780
5	−0.225604	−0.223702	−0.106261	−0.105547
6	−0.224390	−0.223955	−0.109361	−0.108517
7	−0.225144	−0.219250	−0.118561	−0.101741
8	−0.221616	−0.219626	−0.106654	−0.105144
9	−0.231197	−0.226212	−0.114137	−0.109949
10	−0.223527	−0.223418	−0.106841	−0.106827
11	−0.223731	−0.223723	−0.107088	−0.107074

Table S24. Charge transfer analysis for 4.88 GPa (level of theory B97D/6-31+g(d,p))

	Energy (a.u.)			
Pathways	HOMO−1	HOMO	LUMO	LUMO+1
1	−0.192072	−0.192006	−0.115257	−0.115017
2	−0.196656	−0.193404	−0.130861	−0.128453
3	−0.192090	−0.173241	−0.120929	−0.120919
4	−0.187489	−0.179118	−0.136774	−0.108667
5	−0.195427	−0.194084	−0.123659	−0.122971
6	−0.195683	−0.195499	−0.126380	−0.125614
7	−0.194770	−0.191302	−0.135268	−0.119516
8	−0.193419	−0.191637	−0.123904	−0.122400
9	−0.200544	−0.197697	−0.131022	−0.127043
10	−0.195217	−0.195085	−0.124064	−0.124052
11	−0.195402	−0.195396	−0.124376	−0.124364

Table S25. Sum of charge transfer integrals for 1 (for B3LYP and B97D level of theory, respectively).

	H_{AB} (eV)				H_{AB} (eV)		
P (GPa)	hole	electron	Δ	P (GPa)	hole	electron	Δ
0.00	0.50	0.61	0.11	0.00	0.42	0.58	0.16
0.16	0.38	0.64	0.26	0.16	0.30	0.61	0.31
1.09	0.47	0.68	0.22	1.09	0.40	0.65	0.25
2.04	0.50	0.67	0.17	2.04	0.47	0.67	0.20
3.02	0.59	0.72	0.14	3.02	0.50	0.69	0.19
3.96	0.61	0.74	0.13	3.96	0.52	0.71	0.19
4.88	0.66	0.76	0.10	4.88	0.55	0.73	0.18

References for Supporting Information

1. M. J. Cliffe and A. L. Goodwin, *J. Appl. Crystallogr.*, 2012, **45**, 1321–1329.
2. C. Slebodnick, J. Zhao, R. Angel, B. E. Hanson, Y. Song, Z. Liu, and R. J. Hemley, *Inorg. Chem.*, 2004, **43**, 5245–5252.
3. N. P. Funnell, A. Dawson, D. Francis, A. R. Lennie, W. G. Marshall, S. A. Moggach, J. E. Warren, and S. Parsons, *CrystEngComm*, 2010, **12**, 2573–2583.
4. M. I. Aroyo, A. Kirov, C. Capillas, J. M. Perez-Mato, and H. Wondratschek, *Acta Crystallogr. Sect. A*, 2006, **62**, 115–128.
5. Aroyo Mois Ilia, Perez-Mato Juan Manuel, Capillas Cesar, Kroumova Eli, Ivantchev Svetoslav, Madariaga Gotzon, Kirov Asen, and Wondratschek Hans, *Z. Für Krist.*, 2009, **221**, 15.
6. M. I. Aroyo, J. M. Perez-Mato, D. Orobengoa, E. Tasci, G. De La Flor, and A. Kirov, *Bulg. Chem. Commun.*, 2011, **43**, 183–197.
7. A. Gavezzotti, *J. Phys. Chem. B*, 2003, **107**, 2344–2353.
8. A. Gavezzotti, *J. Chem. Theory Comput.*, 2005, **1**, 834–840.
9. A. Gavezzotti, *CrystEngComm*, 2003, **5**, 429–438.